Chemical potential of a test hard sphere of variable size in a hard-sphere fluid

David M. Heyes[1,a)] and Andrés Santos[2,b)]
[1]*Department of Physics, Royal Holloway, University of London, Egham, Surrey TW20 0EX, United Kingdom*
[2]*Departamento de Física and Instituto de Computación Científica Avanzada (ICCAEx), Universidad de Extremadura, E-06071 Badajoz, Spain*

(Received 26 September 2016; accepted 6 November 2016; published online 7 December 2016)

The Labík and Smith Monte Carlo simulation technique to implement the Widom particle insertion method is applied using Molecular Dynamics (MD) instead to calculate numerically the insertion probability, $P_0(\eta, \sigma_0)$, of tracer hard-sphere (HS) particles of different diameters, σ_0, in a host HS fluid of diameter σ and packing fraction, η, up to 0.5. It is shown analytically that the only polynomial representation of $-\ln P_0(\eta, \sigma_0)$ consistent with the limits $\sigma_0 \to 0$ and $\sigma_0 \to \infty$ has necessarily a cubic form, $c_0(\eta) + c_1(\eta)\sigma_0/\sigma + c_2(\eta)(\sigma_0/\sigma)^2 + c_3(\eta)(\sigma_0/\sigma)^3$. Our MD data for $-\ln P_0(\eta, \sigma_0)$ are fitted to such a cubic polynomial and the functions $c_0(\eta)$ and $c_1(\eta)$ are found to be statistically indistinguishable from their exact solution forms. Similarly, $c_2(\eta)$ and $c_3(\eta)$ agree very well with the Boublík–Mansoori–Carnahan–Starling–Leland and Boublík–Carnahan–Starling–Kolafa formulas. The cubic polynomial is extrapolated (high density) or interpolated (low density) to obtain the chemical potential of the host fluid, or $\sigma_0 \to \sigma$, as $\beta\mu^{\text{ex}} = c_0 + c_1 + c_2 + c_3$. Excellent agreement between the Carnahan–Starling and Carnahan–Starling–Kolafa theories with our MD data is evident. *Published by AIP Publishing.* [http://dx.doi.org/10.1063/1.4968039]

I. INTRODUCTION

The statistical mechanical theory of hard-sphere (HS) fluids and solids is important as it underpins the phase behavior and physical properties of a wide range of condensed phase systems such as simple liquids, glasses, colloidal particles, emulsion droplets, and granular materials.[1] This work reports Molecular Dynamics (MD) simulations to test accurate analytical expressions for the chemical potential of a HS impurity of variable diameter at infinite dilution in a HS fluid. This information is a useful precursor for understanding tracer solubility and HS mixtures in general.

We consider a test (or impurity) HS of diameter σ_0 immersed in a sea of HSs of diameter σ at a packing fraction η.[2] The quantity of interest here is the excess chemical potential of the test particle, $\mu_0^{\text{ex}}(\eta, \sigma_0)$, which becomes identical to the excess chemical potential $\mu^{\text{ex}}(\eta)$ of the host fluid in the limit $\sigma_0 \to \sigma$, i.e., $\lim_{\sigma_0 \to \sigma} \mu_0^{\text{ex}}(\eta, \sigma_0) = \mu^{\text{ex}}(\eta)$. As proved by Widom,[3–5] the probability $P_0(\eta, \sigma_0)$ of successful insertion of the test particle is related to the chemical potential through

$$P_0(\eta, \sigma_0) = e^{-\beta\mu_0^{\text{ex}}(\eta, \sigma_0)}, \tag{1.1}$$

where $\beta = 1/k_B T$ and k_B is the Boltzmann constant.

The particle insertion technique has been applied to HS fluids for many decades.[2,3,6–11] However, if η is rather large and $\sigma_0 = \sigma$, the insertion probability is so small that the method becomes inefficient to measure directly $\mu^{\text{ex}}(\eta)$ in computer simulations. In those situations, a circumventing path is needed.

Labík and Smith (LS)[9] proposed a NVT Monte Carlo (MC) simulation technique which can achieve this $\sigma_0 \to \sigma$ limit accurately even at high densities. The method measures the probability of the successful insertion of a solute particle with a range of diameter values, σ_0, smaller than that of the solvent HS diameter. These measurements are extrapolated with a suitable polynomial in powers of σ_0 to $\sigma_0 \to \sigma$, giving the chemical potential of the HS solvent. *Inter alia* they give the tracer chemical potential of the test HS particle of diameter $\sigma_0 < \sigma$. The technique was subsequently extended to fused HS diatomics[10] and HS mixtures.[11]

We note that recently Baranau and Tallarek (BT)[2] applied a solution consisting of measuring the so-called pore-size distribution, fitting it to a Gaussian, and then performing analytically the integral in their Eq. (11) to finally determine the chemical potential. This is an alternative route to the chemical potential of the test particle in the $\sigma_0 \to \sigma$ limit.

In this work, we follow instead the LS method to calculate numerically the insertion probability, $P_0(\eta, \sigma_0)$, for different tracer HS sizes σ_0, in a host HS fluid simulated by MD. The simulation obtained $-\ln P_0(\eta, \sigma_0)$ values are fitted to a cubic polynomial $c_0(\eta) + c_1(\eta)\sigma_0/\sigma + c_2(\eta)(\sigma_0/\sigma)^2 + c_3(\eta)(\sigma_0/\sigma)^3$ (a test function supported by several approximations), and then this polynomial is used to extrapolate (high density) or interpolate (low density) to the value of this quantity at the desired diameter σ. As mentioned above, a bonus from this way is that we obtain the chemical potential $\mu_0(\eta, \sigma_0)$ for a tracer particle with a diameter both smaller and (for some densities) also larger than σ (not only for a fluid particle of the same size as the host fluid HSs). The density-dependent coefficients c_n are

a)Electronic mail: david.heyes@rhul.ac.uk
b)Electronic mail: andres@unex.es. URL: http://www.unex.es/eweb/fisteor/andres/.

also determined, which enables a more detailed comparison with theoretical predictions to be made. Instead of comparing only the chemical potential of the host fluid particle (i.e., $c_0 + c_1 + c_2 + c_3$) as a function of density (as was done, for instance, in Fig. 1(a) of BT's paper), we validate the accuracy of the simulations by (i) confirming agreement with the exact c_0 and c_1 and (ii) comparing two extra coefficients (c_2 and c_3) with literature theoretical predictions, which builds on the pioneering LS work.[9]

The remainder of this paper is organized as follows. The standard theoretical approximations are reviewed in Sec. II, and the use of a cubic polynomial as a trial function for $\beta\mu_0^{\text{ex}}$ is justified. Section III summarizes the Widom particle insertion method and describes the way it is implemented in our MD simulations. The results are presented and compared with theoretical predictions in Sec. IV. Finally, the paper is closed with some conclusions in Sec. V.

II. THEORETICAL APPROXIMATIONS

A. Multi-component hard-sphere fluids

Let us start by considering a (three-dimensional) fluid mixture of additive HSs with an arbitrary number of components. There are N_j spheres of species j having a diameter σ_j, so that the total number of particles is $N = \sum_j N_j$ and the nth moment of the size distribution is

$$M_n = \frac{\sum_j N_j \sigma_j^n}{N}. \tag{2.1}$$

The total packing fraction is

$$\eta = \frac{\pi}{6}\frac{N}{V} M_3, \tag{2.2}$$

where V is the volume of the system.

We will denote the compressibility factor of the mixture by $Z(\eta, \{N_j\}) \equiv pV/Nk_BT$, where p is the pressure. Since its exact form is not known, several approximations have been proposed.[12,13] In particular, the exact solution[14–16] of the Percus–Yevick (PY) integral equation[17] allows one to obtain explicit expressions for $Z(\eta, \{N_j\})$ through different thermodynamic routes. The virial (PY-v), compressibility (PY-c), and chemical-potential (PY-μ) routes in the PY approximation share the following common structure:[14–16,18–20]

$$Z(\eta, \{N_j\}) = Z_0(\eta) + Z_1(\eta)\frac{M_1 M_2}{M_3} + Z_2(\eta)\frac{M_2^3}{M_3^2}, \tag{2.3}$$

where

$$Z_0(\eta) = \frac{1}{1-\eta}, \quad Z_1(\eta) = \frac{3\eta}{(1-\eta)^2}. \tag{2.4}$$

The coefficient $Z_2(\eta)$ depends on the route and several literature predictions are displayed in Table I. On the other hand, the coefficients (2.4) are the same in all the PY approximations. As will be discussed later (see also the Appendix), those coefficients are exact.

Since none of the three prescriptions (PY-v, PY-c, and PY-μ) is particularly accurate, Boublík[21] and, independently, Mansoori *et al.*[22] proposed an interpolation between PY-v and PY-c with respective weights 1/3 and 2/3. The resulting Boublík–Mansoori–Carnahan–Starling–Leland (BMCSL) compressibility factor has of course the structure (2.3) with Z_0 and Z_1 given by Eq. (2.4) and the corresponding expression for Z_2 is also included in Table I. In the monodisperse case (i.e., $\sigma_j \to \sigma \Rightarrow M_n \to \sigma^n$), one has $Z = Z_0 + Z_1 + Z_2$, and the BMCSL equation of state reduces to the Carnahan–Starling (CS) one,[18,23,24]

$$Z_{\text{CS}}(\eta) = \frac{1 + \eta + \eta^2 - \eta^3}{(1-\eta)^3}. \tag{2.5}$$

In 1986, Kolafa proposed a slight correction to the CS equation, namely

$$Z_{\text{CSK}}(\eta) = \frac{1 + \eta + \eta^2 - \frac{2}{3}\eta^3(1+\eta)}{(1-\eta)^3}. \tag{2.6}$$

It first appeared as Eq. (4.46) in a review paper by Boublík and Nezbeda.[25] Following Kolafa's recommendation,[26] we will refer to Eq. (2.6) as the Carnahan–Starling–Kolafa (CSK) equation of state. The extension of Z_{CSK} to mixtures was carried out by Boublík[27] by keeping the structure (2.3) and choosing Z_2 as $Z_2 = Z_{\text{CSK}} - Z_0 - Z_1$. The resulting Boublík–Carnahan–Starling–Kolafa (BCSK) expression is given in the bottom row of Table I.

The excess free energy per particle of the mixture, $a^{\text{ex}}(\eta, \{N_j\})$, is related to the compressibility factor $Z(\eta, \{N_j\})$ through[18]

$$\beta a^{\text{ex}}(\eta, \{N_j\}) = \int_0^1 dt \frac{Z(\eta t, \{N_j\}) - 1}{t}. \tag{2.7}$$

Therefore, the class of approximations of the form (2.3) yield

$$\beta a^{\text{ex}}(\eta, \{N_j\}) = c_0(\eta) + c_1(\eta)\frac{M_1 M_2}{M_3} + a_2(\eta)\frac{M_2^3}{M_3^2}, \tag{2.8}$$

where

$$Z_0(\eta) = 1 + \eta c_0'(\eta) \Rightarrow c_0(\eta) = -\ln(1-\eta), \tag{2.9a}$$

$$Z_1(\eta) = \eta c_1'(\eta) \Rightarrow c_1(\eta) = \frac{3\eta}{1-\eta}, \tag{2.9b}$$

$$Z_2(\eta) = \eta a_2'(\eta) \Rightarrow a_2(\eta) = \int_0^1 dt \frac{Z_2(\eta t)}{t}, \tag{2.9c}$$

the primes denoting derivatives with respect to η. The expressions for the coefficient $a_2(\eta)$ corresponding to the approximations PY-v, PY-c, PY-μ, BMCSL, and BCSK are also included in Table I.

TABLE I. Expressions of $Z_2(\eta)$ [see Eq. (2.3)] and $a_2(\eta)$ [see Eq. (2.8)] according to several approximations.

Approx.	$Z_2(\eta)$	$a_2(\eta)$
PY-v	$\frac{3\eta^2}{(1-\eta)^2}$	$3\ln(1-\eta) + \frac{3\eta}{1-\eta}$
PY-c	$\frac{3\eta^2}{(1-\eta)^3}$	$\frac{3\eta^2}{2(1-\eta)^2}$
PY-μ	$-\frac{9\ln(1-\eta)}{\eta} - 9\frac{1-\frac{3}{2}\eta}{(1-\eta)^2}$	$\frac{9\ln(1-\eta)}{\eta} + 9\frac{1-\frac{1}{2}\eta}{1-\eta}$
BMCSL	$\frac{\eta^2(3-\eta)}{(1-\eta)^3}$	$\ln(1-\eta) + \frac{\eta}{(1-\eta)^2}$
BCSK	$\frac{\eta^2[3-\frac{2}{3}\eta(1+\eta)]}{(1-\eta)^3}$	$\frac{8}{3}\ln(1-\eta)$ $+\eta\frac{16-15\eta+4\eta^2}{6(1-\eta)^2}$

We now consider the excess chemical potential of a generic species i, which is thermodynamically defined as[18]

$$\mu_i^{\rm ex} = \left(\frac{\partial N a^{\rm ex}}{\partial N_i}\right)_{V,N_{j\neq i}}. \tag{2.10}$$

In order to take the derivative in Eq. (2.8), we need to make use of the mathematical properties

$$N\left(\frac{\partial \eta}{\partial N_i}\right)_{V,N_{j\neq i}} = \eta\frac{\sigma_i^3}{M_3}, \tag{2.11a}$$

$$N\left(\frac{\partial NM_1M_2/M_3}{\partial N_i}\right)_{V,N_{j\neq i}} = \frac{M_1M_2}{M_3}\left(\frac{\sigma_i}{M_1}+\frac{\sigma_i^2}{M_2}-\frac{\sigma_i^3}{M_3}\right), \tag{2.11b}$$

$$N\left(\frac{\partial NM_2^3/M_3^2}{\partial N_i}\right)_{V,N_{j\neq i}} = \frac{M_2^3}{M_3^2}\left(3\frac{\sigma_i^2}{M_2}-2\frac{\sigma_i^3}{M_3}\right). \tag{2.11c}$$

Therefore, the final result stemming from Eq. (2.8) is

$$\begin{aligned}\beta\mu_i^{\rm ex}(\eta,\{N_j\}) =& c_0(\eta)+c_1(\eta)\frac{M_1M_2}{M_3}\frac{\sigma_i}{M_1}\\ &+\left[c_1(\eta)\frac{M_1M_2}{M_3}+3a_2(\eta)\frac{M_2^3}{M_3^2}\right]\frac{\sigma_i^2}{M_2}\\ &+\left\{\eta c_0'(\eta)+\left[\eta c_1'(\eta)-c_1(\eta)\right]\frac{M_1M_2}{M_3}\right.\\ &\left.+\left[\eta a_2'(\eta)-2a_2(\eta)\right]\frac{M_2^3}{M_3^2}\right\}\frac{\sigma_i^3}{M_3}.\end{aligned} \tag{2.12}$$

Note that Eqs. (2.3), (2.8), and (2.12) are consistent with the exact thermodynamic relation

$$\frac{1}{N}\sum_i N_i\beta\mu_i^{\rm ex} = \beta a^{\rm ex}+Z-1, \tag{2.13}$$

thanks to the properties in (2.9), regardless of the expression for $a_2(\eta)$.

As proved in the Appendix (where a general dimensionality d is considered), Eq. (2.12) is *exact* to first order in σ_i, i.e.,

$$\beta\mu_i^{\rm ex}(\eta,\{N_j\}) = c_0(\eta)+c_1(\eta)\frac{M_1M_2}{M_3}\frac{\sigma_i}{M_1}+\mathcal{O}(\sigma_i^2). \tag{2.14}$$

This in turn proves the exact character of the coefficients c_0 and c_1 in Eqs. (2.9a) and (2.9b), respectively, and, hence, of the coefficients Z_0 and Z_1 in Eq. (2.4), as anticipated before.

B. Test particle in a one-component hard-sphere fluid

In this special case, we can set $M_n \to \sigma^n$ and particularize Eq. (2.12) to a species $i=0$ made of a single particle of diameter σ_0. The result is

$$\beta\mu_0^{\rm ex}(\eta,\sigma_0) = c_0(\eta)+c_1(\eta)\frac{\sigma_0}{\sigma}+c_2(\eta)\frac{\sigma_0^2}{\sigma^2}+c_3(\eta)\frac{\sigma_0^3}{\sigma^3}, \tag{2.15}$$

where

$$c_2(\eta) = c_1(\eta)+3a_2(\eta), \tag{2.16a}$$

$$c_3(\eta) = \eta c_0'(\eta)+\eta c_1'(\eta)-c_1(\eta)+\eta a_2'(\eta)-2a_2(\eta). \tag{2.16b}$$

Notice that from Eqs. (2.9) and (2.16) one can obtain the simple relation[9]

$$c_3(\eta) = Z(\eta)-1-\frac{1}{3}c_1(\eta)-\frac{2}{3}c_2(\eta). \tag{2.17}$$

Inserting Eqs. (2.9a) and (2.9b) together with the approximate expressions of a_2 listed in Table I into Eq. (2.16), one can obtain the approximate expressions for the coefficients c_2 and c_3 given in Table II. The last column of Table II presents formulas for the excess chemical potential of the fluid, i.e., $\beta\mu^{\rm ex}(\eta) = \lim_{\sigma_0\to 1}\beta\mu_0^{\rm ex}(\eta,\sigma_0) = c_0(\eta)+c_1(\eta)+c_2(\eta)+c_3(\eta)$, for the various approximations.

Given that a number of approximations (PY-v, PY-c, PY-μ, BMCSL, and BCSK) share the common cubic polynomial form (2.15) (with the exact coefficients c_0 and c_1) for the excess chemical potential of a test particle immersed in a monodisperse HS fluid, one might reasonably query whether one could construct either a simpler approximation (with adjustable c_2) from a quadratic polynomial or a more accurate approximation (with adjustable c_2, c_3, c_4, ...) from a polynomial of degree higher than three. However, as we will see, if $\beta\mu_0^{\rm ex}(\eta,\sigma_0)$ is represented by a polynomial in the diameter σ_0, the polynomial must *necessarily* be of third degree. This is a consequence of the physical requirement that, in the limit of an infinitely large impurity, one must have[28–30]

$$\eta Z(\eta) = \lim_{\sigma_0\to\infty}\frac{\beta\mu_0^{\rm ex}(\eta,\sigma_0)}{(\sigma_0/\sigma)^3}. \tag{2.18}$$

Therefore, since $\lim_{\sigma_0\to\infty}\beta\mu_0^{\rm ex}(\eta,\sigma_0)/\sigma_0^3$ can be neither zero nor infinity, the only polynomial approximations consistent with that property are third-degree ones.

In the case of the approximations of the form (2.3), Eq. (2.18) implies

$$c_3(\eta) = \eta Z(\eta) = \eta\left[Z_0(\eta)+Z_1(\eta)+Z_2(\eta)\right]. \tag{2.19}$$

TABLE II. Expressions of $c_2(\eta)$, $c_3(\eta)$ [see Eq. (2.15)], and $\beta\mu^{\rm ex}(\eta)$ according to several approximations.

Approx.	$c_2(\eta)$	$c_3(\eta)$	$\beta\mu^{\rm ex}(\eta)$
PY-v	$9\ln(1-\eta)+12\frac{\eta}{1-\eta}$	$-6\ln(1-\eta)-\eta\frac{5-11\eta}{(1-\eta)^2}$	$2\ln(1-\eta)+2\eta\frac{5-2\eta}{(1-\eta)^2}$
PY-c	$3\eta\frac{2+\eta}{2(1-\eta)^2}$	$\eta\frac{1+\eta+\eta^2}{(1-\eta)^3}$	$-\ln(1-\eta)+\eta\frac{14-13\eta+5\eta^2}{2(1-\eta)^3}$
PY-μ	$27\frac{\ln(1-\eta)}{\eta}+3\frac{18-7\eta}{2(1-\eta)}$	$-27\frac{\ln(1-\eta)}{\eta}-\frac{54-83\eta+14\eta^2}{2(1-\eta)^2}$	$-\ln(1-\eta)+\eta\frac{14+\eta}{2(1-\eta)^2}$
BMCSL	$3\ln(1-\eta)+3\eta\frac{2-\eta}{(1-\eta)^2}$	$-2\ln(1-\eta)-\eta\frac{1-6\eta+3\eta^2}{(1-\eta)^3}$	$\eta\frac{8-9\eta+3\eta^2}{(1-\eta)^3}$
BCSK	$8\ln(1-\eta)+\eta\frac{22-21\eta+4\eta^2}{2(1-\eta)^2}$	$-\frac{16}{3}\ln(1-\eta)-\eta\frac{13-43\eta+27\eta^2-2\eta^3}{3(1-\eta)^3}$	$\frac{5}{3}\ln(1-\eta)+\eta\frac{58-79\eta+39\eta^2-8\eta^3}{6(1-\eta)^3}$

It can be noticed that Eq. (2.19) is independent of Eq. (2.17). In fact, it can be easily checked that the PY-v, PY-μ, BMCSL, and BCSK expressions for $Z_2(\eta)$ (see Table I) and $c_3(\eta)$ (see Table II) are inconsistent with Eq. (2.19). This means that those approximations qualitatively agree with the physical requirement (2.18) in that $\lim_{\sigma_0\to\infty}\beta\mu_0^{\text{ex}}(\eta,\sigma_0)/\sigma_0^3 =$ finite but yield different results for the left- and right-hand sides. On the other hand, the PY-c approximation, which actually is equivalent to the Scaled Particle Theory (SPT) approximation,[31–35] is fully consistent with Eqs. (2.18) and (2.19). As a matter of fact, the PY-c/SPT cubic prescription for $\beta\mu_0^{\text{ex}}(\eta,\sigma_0)$ is the only one that is simultaneously consistent with both Eqs. (2.17) and (2.19) without violating the value $b_3 = 10$ for the third virial coefficient of the one-component fluid. The combination of Eqs. (2.17) and (2.19) [together with Eqs. (2.9) and (2.16a)] yields the differential equation $a_2'(\eta) = 2a_2(\eta)/\eta(1-\eta)$, whose general solution is $a_2(\eta) = K\eta^2/(1-\eta)^2$, K being a constant. The associated third virial coefficient is $b_3 = 7 + 2K$, so that $b_3 = 10$ implies $K = \frac{3}{2}$ and thus one recovers the PY-c/SPT approximation.

Section III describes the process and results of a MD simulation study of this HS system which were carried out to help determine which of the approximations for c_2 and c_3 (see Table II) is best.

III. WIDOM'S PARTICLE INSERTION METHOD AND MOLECULAR DYNAMICS SIMULATION

Consider an N-particle system where $\Phi_N(\mathbf{r}^N)$ is the potential energy. The Widom particle insertion method for the excess chemical potential μ^{ex} is[3,6,36,37]

$$e^{-\beta\mu^{\text{ex}}} = \frac{\int d\mathbf{r}^{N+1}\, e^{-\beta\Phi_N(\mathbf{r}^N)} e^{-\beta\Delta\Phi_{N+1}(\mathbf{r}^{N+1})}}{V\int d\mathbf{r}^N\, e^{-\beta\Phi_N(\mathbf{r}^N)}} = \left\langle e^{-\beta\Delta\Phi_{N+1}(\mathbf{r}^{N+1})}\right\rangle, \tag{3.1}$$

where $\Delta\Phi_{N+1}(\mathbf{r}^{N+1}) = \Phi_{N+1}(\mathbf{r}^{N+1}) - \Phi_N(\mathbf{r}^N)$ and the ensemble average is denoted by $\langle\cdots\rangle$. The $(N+1)$th particle (here denoted by the subscript 0) can be considered to be a test particle, as it does not influence the physical distribution of the other N particles. Hence,

$$\beta\mu_0^{\text{ex}} = -\ln\left\langle e^{-\beta\Delta\Phi_{N+1}(\mathbf{r}^{N+1})}\right\rangle. \tag{3.2}$$

The test particle is inserted randomly into the N-particle host fluid. The important point is that it does so in a non-intrusive way. For HSs, Eq. (3.2) reduces to a simple bookkeeping procedure as $\exp(-\beta\Delta\Phi_{N+1})$ either is 1 when the test sphere does not overlap with any of the N particles or is equal to 0 if it overlaps with any of them. As discussed in Sec. II, the test particle does not need to be the same type of particle as the other N particles. We consider the particle $\alpha = 0$ to be an impurity HS of diameter σ_0, taking the HS diameter of the host fluid to be σ.

Our numerical implementation of the Widom insertion method run as follows. At a given packing fraction η, a monodisperse HS fluid was simulated by a standard MD method. The procedure was to randomly insert a test "point" in the system and calculate the distance r_n from that point to the center of the nearest sphere. Then, all the values from $\sigma_0 = 0$ to $\sigma_0 = 2r_n - \sigma$ represented accepted insertions, which were accumulated efficiently in a histogram at the same time in the MD simulation. In addition, as the test particles are introduced in a non-intrusive way, many of them can be inserted at the same time, and we used the same number of test particles as the number of host fluid particles. One difference with the LS method[9] is that we use MD rather than MC to evolve the host fluid assembly of HSs.

For each trial insertion r_n, 1 was added to all entrants of a histogram (rather like that for the radial distribution function) for $P_0(\eta,\sigma_0)$, for $\sigma_0 = 2r_n - \sigma$ and all σ_0 values less than $2r_n - \sigma$ at the same time. This is a statistically efficient procedure for computing the chemical potential of the impurity at infinite dilution, $\beta\mu_0^{\text{ex}}(\eta,\sigma_0)$. The chemical potential of the HS fluid is just $\mu^{\text{ex}}(\eta) = \mu_0^{\text{ex}}(\eta,\sigma)$ when $\sigma_0 = \sigma$. At not too high densities, data on the chemical potential for $\sigma_0 > \sigma$ can also be obtained, and so the HS chemical potential becomes a matter of interpolation and data fitting in that case. For states near a packing fraction $\eta \approx 0.50$, the HS chemical potential needs to be estimated by the extrapolation of the $\sigma_0 < \sigma$ histogram entrants, as the probability of inserting a HS in a HS fluid during a typical simulation can be impracticably small (less than 10^{-7}).

At each density, the MD values of $\beta\mu_0(\eta,\sigma_0)$ as a function of σ_0 were fitted to the cubic polynomial (2.15) to obtain the four coefficients c_0–c_3, without imposing the exact values (2.9a) and (2.9b) of c_0 and c_1. This contrasts with the LS procedure,[9] where the coefficients c_0 and c_1 were fixed to be given by Eqs. (2.9a) and (2.9b), the coefficient c_3 was forced to satisfy the relationship (2.17) (with Z obtained by independent MC simulations of the host fluid), and therefore only the coefficient c_2 was fitted to the simulation data of $-\ln P_0(\eta,\sigma_0)$. In addition, the maximum value of σ_0 used in the least-square fitting corresponded to[9] $P_0 \approx 10^{-3}$.

Our simulations were carried out with $N = 2048$ HSs. There were ca. 1.4×10^5 collisions per particle at $\eta = 0.05$ and 5.6×10^5 collisions per particle at $\eta = 0.5$. The maximum value of σ_0 chosen for the fitting process was 1.10σ, for $\eta < 0.4$, decreasing to 0.90σ for $\eta = 0.46$ to 0.80σ for $\eta \geq 0.48$. This corresponded to $P_0 \approx 2\times10^{-5}$. The insertion probability histogram had a resolution of 0.005σ.

IV. RESULTS

Figure 1 shows the values of $\beta\mu_0^{\text{ex}}(\eta,\sigma_0)$ obtained in our simulations for nine representative packing fractions from $\eta = 0.05$ to $\eta = 0.50$. The least-square fits to a cubic polynomial are also included in Fig. 1 and an excellent agreement is found.

The extracted values of the coefficients $c_0(\eta)$ and $c_1(\eta)$ are plotted in Fig. 2 for 31 values of η ranging from 0.05 to 0.50. Comparison with the exact expressions (2.9a) and (2.9b) shows an extremely good agreement. This confirms and reinforces the reliability and accuracy of our MD results.

Figure 3 displays the values of the fitted coefficients $c_2(\eta)$ and $c_3(\eta)$ for the same densities as in Fig. 2. Since the exact expressions of c_2 and c_3 are (to the best of our knowledge) unknown, we compare the simulation values with the

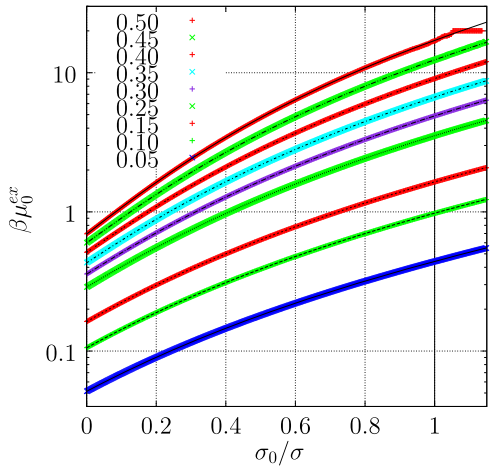

FIG. 1. Plot of the excess chemical potential of a test particle, $\beta\mu_0^{\rm ex}(\eta,\sigma_0)$, as a function of the diameter σ_0. The symbols are the values obtained in our MD simulations by the Widom insertion method, while the lines are least-square fits to cubic polynomials of the form (2.15) with free coefficients c_n. The noisiest data for large η and σ_0 were excluded from the fits. The different values of η are indicated in the legend.

approximate theoretical predictions considered in Table II. Up to $\eta \simeq 0.2$, all the theories practically overlap and reproduce the MD values. At higher densities, however, the three PY predictions clearly deviate from the simulation data: while the PY-c approximation overestimates the data, the PY-μ and, especially, the PY-v approximations underestimate them. On

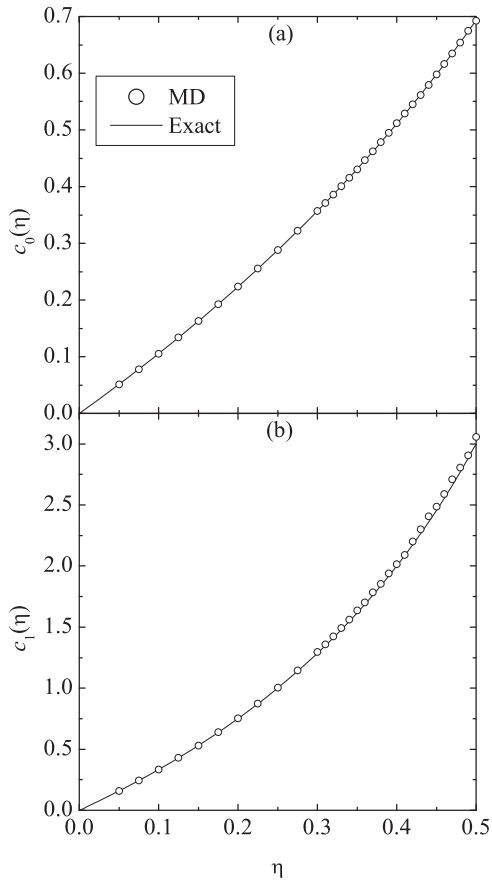

FIG. 2. Plot of the coefficients (a) $c_0(\eta)$ and (b) $c_1(\eta)$. The lines represent the exact expressions [see Eqs. (2.9a) and (2.9b)], while the symbols represent the values obtained from a least-square fit of MD data.

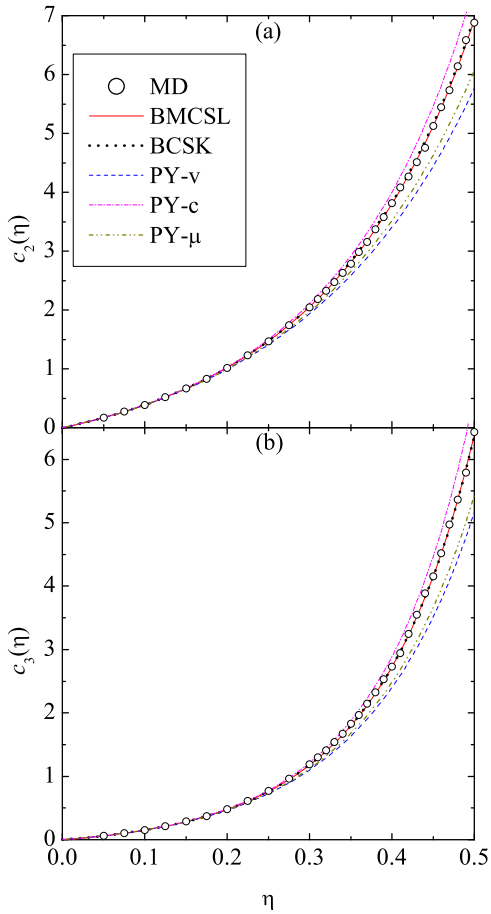

FIG. 3. Plot of the coefficients (a) $c_2(\eta)$ and (b) $c_3(\eta)$. The lines represent the theoretical expressions (see Table II), while the symbols represent the values obtained from a least-square fit of MD data.

the other hand, the BMCSL and BCSK curves, which are practically indistinguishable, reproduce excellently the MD results.

Now that we have validated our numerical values of the four coefficients c_n characterizing the diameter dependence of the impurity chemical potential $\beta\mu_0^{\rm ex}$, an accurate estimate of the chemical potential of the pure HS fluid, written as $\beta\mu^{\rm ex} = c_0 + c_1 + c_2 + c_3$, can be made. The results are shown in Fig. 4(a), where they are compared with the PY, CS, and CSK approximations (see again Table II). The observed trends are similar to those presented in Fig. 3. In particular, there is excellent agreement between the present MD results and the CS and CSK theories. Figure 4(a) also includes the MC data reported in Ref. 9, which are fully consistent with our MD results.

An interesting additional feature of our approach is that we can predict the compressibility factor $Z(\eta)$ of the HS fluid via Eq. (2.17) from the knowledge of the coefficients c_n characterizing the size dependence of the solute chemical potential $\beta\mu_0^{\rm ex}$, i.e., $Z = 1 + \frac{1}{3}c_1 + \frac{2}{3}c_2 + c_3$. This quantity is plotted in Fig. 4(b), where it shows again an excellent agreement with the CS and CSK approximations, as well as with the results obtained in Ref. 9 directly from MC simulations of the radial distribution function at contact.

In principle, one could also estimate Z only from c_3 as $Z = c_3/\eta$ [see Eq. (2.19)]. As shown in Fig. 4(b), the values

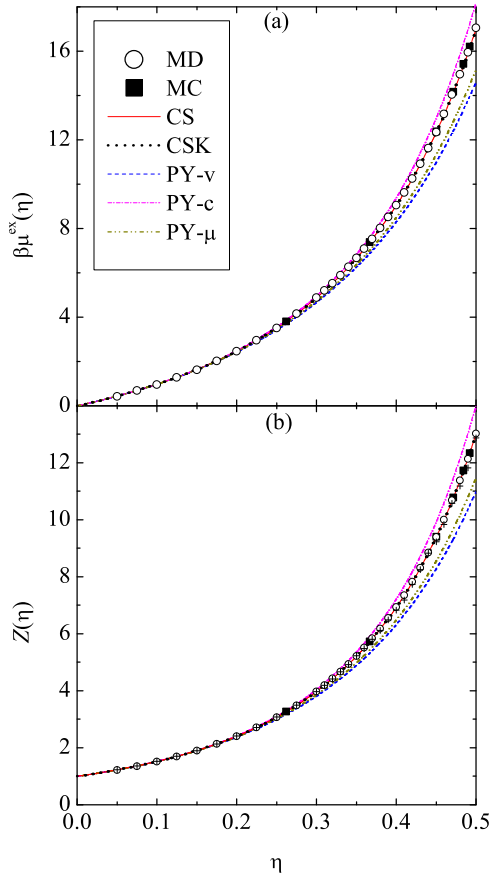

FIG. 4. Plot of (a) the excess chemical potential $\beta\mu^{\rm ex}(\eta)$ and (b) the compressibility factor $Z(\eta)$. The lines represent the theoretical expressions (see Tables I and II), the open circles represent $\beta\mu^{\rm ex} = c_0 + c_1 + c_2 + c_3$ and $Z = 1 + \frac{1}{3}c_1 + \frac{2}{3}c_2 + c_3$ (with coefficients c_n obtained from a least-square fit of our MD data), and the filled squares represent the MC data of Ref. 9. In panel (b), the crosses represent c_3/η.

of c_3/η agree very well with those of $1 + \frac{1}{3}c_1 + \frac{2}{3}c_2 + c_3$ up to $\eta \simeq 0.35$, but tend to lie slightly below the latter ones at higher densities. This small discrepancy is just a consequence of the fact that the *exact* function $\beta\mu_0^{\rm ex}(\eta, \sigma_0)$ is *not* a cubic polynomial. In fact, as discussed at the end of Sec. II, the only cubic polynomial that is consistent with both Eqs. (2.17) and (2.19) is the PY-c/SPT approximation, which is not particularly accurate. Our MD results show that the excess chemical potential $\beta\mu_0^{\rm ex}(\eta, \sigma_0)$ can be fitted extremely well by a cubic polynomial for diameters σ_0 from $\sigma_0 = 0$ to $\sigma_0 \sim \sigma$ (see Fig. 1). On the other hand, while the choice of the degree of the polynomial is consistent with the exact property $\lim_{\sigma_0\to\infty}\beta\mu_0^{\rm ex}(\eta, \sigma_0)/(\sigma_0/\sigma)^3 =$ finite, it would be too far-fetched to expect that such an extreme limit coincides with the coefficient c_3 fitted in the range $0 \le \sigma_0 \lesssim \sigma$. The fact, however, that the coefficient c_3 is so close to ηZ means that the cubic polynomial fitted in the range $0 \le \sigma_0 \lesssim \sigma$ keeps being a very good approximation even if $\sigma_0 \gg \sigma$. Anyway, the recommended route to measure the compressibility factor from a fit of the form (2.15) for $\sigma_0 \lesssim \sigma$ is $Z = 1 + \frac{1}{3}c_1 + \frac{2}{3}c_2 + c_3$ rather than $Z = c_3/\eta$.

For future reference of researchers interested in the chemical potential of HS fluids, we present in Table III the numerical values of the MD data plotted in Figs. 2–4.

TABLE III. Numerical values of $c_0, c_1, c_2, c_3, \beta\mu^{\rm ex} = c_0 + c_1 + c_2 + c_3$, and $Z = 1 + \frac{1}{3}c_1 + \frac{2}{3}c_2 + c_3$, as obtained from our MD simulations. The errors in the constants c_0–c_3 range from 0.002% to 0.01% at $\eta = 0.075$ to 0.06%–0.15% at $\eta = 0.50$.

η	c_0	c_1	c_2	c_3	$\beta\mu^{\rm ex}$	Z
0.050	0.051 38	0.157 91	0.170 53	0.061 32	0.4411	1.2276
0.075	0.078 07	0.243 63	0.272 51	0.102 32	0.6965	1.3652
0.100	0.105 51	0.334 13	0.387 26	0.152 54	0.9794	1.5221
0.125	0.133 71	0.429 76	0.517 31	0.213 00	1.2938	1.7011
0.150	0.162 77	0.530 66	0.665 23	0.285 45	1.6441	1.9058
0.175	0.192 64	0.638 53	0.830 44	0.374 40	2.0360	2.1409
0.200	0.223 40	0.753 38	1.016 29	0.482 54	2.4756	2.4112
0.225	0.255 19	0.875 20	1.229 27	0.611 28	2.9709	2.7225
0.250	0.288 02	1.005 69	1.468 54	0.768 83	3.5311	3.0831
0.275	0.321 90	0.145 94	1.738 17	0.960 82	4.1668	3.5016
0.300	0.356 94	1.296 67	2.045 55	1.193 20	4.8924	3.9891
0.310	0.371 34	0.359 32	2.182 12	1.297 33	5.2101	4.2052
0.320	0.385 94	1.423 89	2.325 56	1.412 04	5.5474	4.4370
0.330	0.400 65	1.492 84	2.471 22	1.538 68	5.9034	4.6838
0.340	0.415 82	1.560 42	2.632 06	1.672 37	6.2807	4.9472
0.350	0.430 65	1.637 51	2.783 36	1.829 38	6.6809	5.2308
0.360	0.446 64	1.703 77	2.981 53	1.970 59	7.1025	5.5262
0.370	0.462 10	1.783 29	3.157 55	2.147 89	7.5508	5.8473
0.380	0.478 63	1.855 19	3.371 50	2.323 90	8.0292	6.1900
0.390	0.494 64	1.939 13	3.574 37	2.528 17	8.5363	6.5575
0.400	0.511 57	2.016 26	3.816 78	2.728 71	9.0733	6.9453
0.410	0.529 23	2.091 01	4.083 54	2.943 10	9.6469	7.3625
0.420	0.544 83	2.202 51	4.269 02	3.248 96	10.265	7.8291
0.430	0.561 75	2.301 81	4.511 57	3.548 99	10.924	8.3240
0.440	0.578 97	2.407 85	4.757 77	3.884 09	11.629	8.8586
0.450	0.598 08	2.487 43	5.127 05	4.155 86	12.368	9.4030
0.460	0.616 55	2.589 68	5.443 13	4.522 32	13.172	10.014
0.470	0.634 62	2.710 22	5.730 96	4.972 55	14.048	10.697
0.480	0.654 43	2.807 28	6.141 40	5.365 83	14.969	11.396
0.490	0.674 73	2.907 78	6.582 17	5.790 39	15.955	12.148
0.500	0.692 85	3.057 78	6.878 40	6.433 86	17.063	13.039

V. CONCLUSIONS

To conclude, this work provides new insights into the properties of the chemical potential of HS fluids and its relation with the equation of state. A third-degree expression in the test particle diameter for the chemical potential is shown to reproduce well that for HSs with the same diameter as those of the host fluid, and also for those tracer particles with smaller and, to some extent, larger diameters (not too close to $\eta = 0.49$ in the latter case). It is found that the chemical potential predicted by the CS and the CSK equations is in close agreement with simulation data. However, it is concluded that although a third-degree polynomial in the tracer particle diameter is a very good approximation of the chemical potential, this functional form cannot be exact. It is also shown that the equation of state of the HS fluid can be accurately obtained from the polynomial fit of the simulation data for the chemical potential.

Originally implemented on NVT MC simulations, we have applied in this paper the LS technique[9] to MD simulations. In addition, our implementation differs from that of Ref. 9 in a few aspects. First, all four coefficients c_0–c_3 have been fitted, whereas LS forced c_0 and c_1 to be equal to their exact values and enslaved c_3 to c_2 by means of Eq. (2.17), so

that in the end only the coefficient c_2 was fitted. Also, they needed to measure the compressibility factor Z (from the contact value of the radial distribution function) independently of the insertion probability measurements, whereas in our case Z is just another output (in addition to $\beta\mu^{\rm ex}$) rather than an input. The excellent agreement between the fitted c_0 and c_1 with the exact expressions is an *a posteriori* confirmation of the accuracy of the results reported in this paper. We have been able to reach reliable statistical results up to $P_0 \approx 2\times 10^{-5}$, which is about 50 times smaller than the threshold value considered in Ref. 9. Furthermore, our study covers a much larger number of densities.

The LS simulation technique is shown to be an extremely powerful and adaptable tool to obtain the chemical potential of tracer particles and the equation of state of HS fluids. It has also been shown that the BMCSL and BCSK formulas for c_2 and c_3 are extremely accurate and not distinguishable from the numerical data. Therefore, it may be concluded that the equation of state of the monodisperse HS fluid can be considered for *most* practical *applications* to be a solved analytical problem.

In the extension to HS binary mixtures of the LS method carried out by Barošová *et al.*,[11] the authors fitted their MC simulated values of $P_0(\eta,\sigma_0)$ to a quartic polynomial. On the other hand, we plan to extend our MD implementation to HS mixtures (binary, ternary, or, more generally, polydisperse) by keeping instead a cubic form since the exact condition $\lim_{\sigma_0\to\infty}\beta\mu_0^{\rm ex}(\eta,\sigma_0)/\sigma_0^3 =$ finite still holds for mixtures. According to Eq. (2.12), the coefficient c_0 is the same as in the monodisperse system, while the linear coefficient, once multiplied by M_3/M_1M_2, is again the exact c_1. As carried out in the present paper, these two conditions will be used as confidence tests of the simulation results.

ACKNOWLEDGMENTS

The research of A.S. has been partially supported by the Spanish Government through Grant No. FIS2013-42840-P and by the Regional Government of Extremadura (Spain) through Grant No. GR15104 (partially financed by ERDF funds). D.M.H. would like to thank Dr. T. Crane (Department of Physics, Royal Holloway, University of London, UK) for helpful software support.

APPENDIX: CHEMICAL POTENTIAL IN THE SMALL-SIZE LIMIT

We consider an N-particle HS mixture in d dimensions. The packing fraction of the mixture is $\eta = (N/V)v_dM_d$, where $v_d = (\pi/4)^{d/2}/\Gamma(1+d/2)$ is the volume occupied by a sphere of unit diameter. The Boltzmann factor associated with the potential energy $\Phi_N(\mathbf{r}^N)$ of the mixture is

$$e^{-\beta\Phi_N(\mathbf{r}^N)} = \prod_{\alpha=1}^{N-1}\prod_{\gamma=\alpha+1}^{N}\Theta\left(r_{\alpha\gamma}-\sigma_{\ell_\alpha\ell_\gamma}\right), \tag{A1}$$

where $\Theta(x)$ is the Heaviside step function, $r_{\alpha\gamma} = |\mathbf{r}_\alpha - \mathbf{r}_\gamma|$ is the relative distance between particles α and γ, ℓ_α denotes the species particle α belongs to, and $\sigma_{ij} = \frac{1}{2}(\sigma_i+\sigma_j)$.

Now we assume that an extra test particle of diameter σ_0 is inserted into the fluid. The canonical ensemble expression for the insertion probability is [see Eq. (3.1)]

$$P_0(\eta,\sigma_0) = \left\langle\prod_{\gamma=1}^{N}\Theta(r_{0\gamma}-\sigma_{0\ell_\gamma})\right\rangle = \frac{\int d\mathbf{r}^N\, e^{-\beta\Phi_N(\mathbf{r}^N)}\int d\mathbf{r}_0\prod_{\gamma=1}^{N}\Theta(r_{0\gamma}-\sigma_{0\ell_\gamma})}{V\int d\mathbf{r}^N\, e^{-\beta\Phi_N(\mathbf{r}^N)}}. \tag{A2}$$

In the limit $\sigma_0\to 0$, we can write

$$P_0(\eta,\sigma_0) = P_0(\eta,0) + \dot{P}_0(\eta,0)\sigma_0 + \mathcal{O}(\sigma_0^2), \tag{A3}$$

where the dot denotes a derivative with respect to σ_0. The first term on the right-hand side of Eq. (A3) is trivial since

$$\int d\mathbf{r}_0\prod_{\gamma=1}^{N}\Theta\left(r_{0\gamma}-\frac{\sigma_{\ell_\gamma}}{2}\right) = V(1-\eta). \tag{A4}$$

This expresses the fact that, for any nonoverlapping configuration of N spheres, the available volume for the test point particle is $V(1-\eta)$. Consequently,

$$P_0(\eta,0) = 1-\eta. \tag{A5}$$

As for the derivative $\dot{P}_0(\eta,\sigma_0)$, it is given from Eq. (A2) by

$$\dot{P}_0(\eta,\sigma_0) = -\frac{1}{2}\sum_{\alpha=1}^{N}\frac{\int d\mathbf{r}^N\, e^{-\Phi_N(\mathbf{r}^N)}\int d\mathbf{r}_0\,\delta(r_{0\alpha}-\sigma_{0\ell_\alpha})\prod_{\gamma\neq\alpha}\Theta(r_{0\gamma}-\sigma_{0\ell_\gamma})}{V\int d\mathbf{r}^N\, e^{-\beta\Phi_N(\mathbf{r}^N)}}. \tag{A6}$$

Making $\sigma_0\to 0$ and assuming again a nonoverlapping configuration of the fluid particles, we can write

$$\int d\mathbf{r}_0\;\delta\left(r_{0\alpha}-\frac{\sigma_{\ell_\alpha}}{2}\right)\prod_{\gamma\neq\alpha}\Theta\left(r_{0\gamma}-\frac{\sigma_{\ell_\gamma}}{2}\right) = \Omega_d\lim_{\epsilon\to 0}\int_0^{\frac{\sigma_{\ell_\alpha}}{2}+\epsilon} dr_{0\alpha}\, r_{0\alpha}^{d-1}\delta\left(r_{0\alpha}-\frac{\sigma_{\ell_\alpha}}{2}\right) = \Omega_d 2^{1-d}\sigma_{\ell_\alpha}^{d-1}, \tag{A7}$$

where $\Omega_d = dv_d2^d$ is the total solid angle. Therefore,

$$\dot{P}_0(\eta,0) = -d\eta\frac{M_{d-1}}{M_d}. \tag{A8}$$

After insertion of Eqs. (A5) and (A8), Eq. (A3) becomes

$$P_0(\eta,\sigma_0) = (1-\eta)\left(1 - d\frac{\eta}{1-\eta}\frac{M_1 M_{d-1}}{M_d}\frac{\sigma_0}{M_1}\right) + \mathcal{O}(\sigma_0^2). \quad \text{(A9)}$$

Finally, from Eq. (1.1) we find

$$\beta\mu_0^{\text{ex}}(\eta,\sigma_0) = c_0(\eta) + c_1(\eta)\frac{M_1 M_{d-1}}{M_d}\frac{\sigma_0}{M_1} + \mathcal{O}(\sigma_0^2), \quad \text{(A10)}$$

with

$$c_0(\eta) = -\ln(1-\eta), \quad c_1(\eta) = d\frac{\eta}{1-\eta}. \quad \text{(A11)}$$

Identifying the test particle as a particle of species i (i.e., $\sigma_0 = \sigma_i$) and focusing on $d = 3$, it can be readily shown that Eqs. (A10) and (A11) reduce to Eqs. (2.14) and (2.9a) and (2.9b), respectively.

Equation (A8) can be obtained by a different route. Imagine a test particle that can (partially) "penetrate" inside the fluid particles, i.e., it has a *nominal* diameter $\sigma_0 < 0$ so that the closest distance σ_{0j} between the centers of the test particle and a particle of species j is smaller than $\frac{1}{2}\sigma_j$. In that case, Eq. (A2) still holds and, in analogy to Eq. (A4),

$$\int d\mathbf{r}_0 \prod_{\gamma=1}^{N} \Theta(r_{0\gamma} - \sigma_{0\ell_\gamma}) = V - \sum_j N_j v_d (2\sigma_{0j})^d. \quad \text{(A12)}$$

Therefore,

$$P_0(\eta,\sigma_0<0) = 1 - \frac{1}{V}\sum_j N_j v_d(\sigma_0+\sigma_j)^d, \quad \text{(A13a)}$$

$$\dot{P}_0(\eta,\sigma_0<0) = -\frac{d}{V}\sum_j N_j v_d(\sigma_0+\sigma_j)^{d-1}. \quad \text{(A13b)}$$

Taking the limit $\sigma_0 \to 0$, Eqs. (A13) reduce to Eqs. (A5) and (A8). This in turn shows that both $P_0(\eta,\sigma_0)$ and $\dot{P}_0(\eta,\sigma_0)$ are continuous at $\sigma_0 = 0$.

[1] *Theory and Simulation of Hard-Sphere Fluids and Related Systems*, Vol. 753, edited by A. Mulero (Springer-Verlag, Berlin, 2008).
[2] V. Baranau and U. Tallarek, J. Chem. Phys. **144**, 214503 (2016).
[3] B. Widom, J. Chem. Phys. **39**, 2808 (1963).
[4] K. S. Shing and K. E. Gubbins, Mol. Phys. **43**, 717 (1981).
[5] G. L. Deitrick, L. E. Scriven, and H. T. Davis, J. Chem. Phys. **90**, 2370 (1989).
[6] W. G. Hoover and J. C. Poirier, J. Chem. Phys. **37**, 1041 (1962).
[7] I. Nezbeda and J. Kolafa, Mol. Simul. **5**, 391 (1991).
[8] P. Attard, J. Chem. Phys. **98**, 2225 (1993).
[9] S. Labík and W. R. Smith, Mol. Simul. **12**, 23 (1994).
[10] S. Labík, V. Jirásek, A. Malijevský, and W. Smith, Chem. Phys. Lett. **247**, 227 (1995).
[11] M. Barošová, A. Malijevský, S. Labík, and W. R. Smith, Mol. Phys. **87**, 423 (1996).
[12] A. Mulero, C. A. Galán, M. I. Parra, and F. Cuadros, in *Theory and Simulation of Hard-Sphere Fluids and Related Systems*, Vol. 753, edited by A. Mulero (Springer-Verlag, Berlin, 2008), pp. 37–109.
[13] C. Barrio and J. R. Solana, in *Theory and Simulation of Hard-Sphere Fluids and Related Systems*, Vol. 753, edited by A. Mulero (Springer-Verlag, Berlin, 2008), pp. 133–182.
[14] J. L. Lebowitz and D. Zomick, J. Chem. Phys. **54**, 3335 (1971).
[15] J. W. Perram and E. R. Smith, Chem. Phys. Lett. **35**, 138 (1975).
[16] B. Barboy, Chem. Phys. **11**, 357 (1975).
[17] J. K. Percus and G. J. Yevick, Phys. Rev. **110**, 1 (1958).
[18] A. Santos, *A Concise Course on the Theory of Classical Liquids: Basics and Selected Topics*, Vol. 923 (Springer, New York, 2016).
[19] A. Santos, Phys. Rev. Lett. **109**, 120601 (2012).
[20] A. Santos and R. D. Rohrmann, Phys. Rev. E **87**, 052138 (2013).
[21] T. Boublík, J. Chem. Phys. **53**, 471 (1970).
[22] G. A. Mansoori, N. F. Carnahan, K. E. Starling, and J. T. W. Leland, J. Chem. Phys. **54**, 1523 (1971).
[23] N. F. Carnahan and K. E. Starling, J. Chem. Phys. **51**, 635 (1969).
[24] D. M. Heyes, M. J. Cass, J. G. Powles, and W. A. B. Evans, J. Phys. Chem. B **111**, 1455 (2007).
[25] T. Boublík and I. Nezbeda, Collect. Czech. Chem. Commun. **51**, 2301 (1986).
[26] J. Kolafa, private communication (1998).
[27] T. Boublík, Mol. Phys. **59**, 371 (1986).
[28] H. Reiss, H. L. Frisch, E. Helfand, and J. L. Lebowitz, J. Chem. Phys. **32**, 119 (1960).
[29] R. Roth, R. Evans, A. Lang, and G. Kahl, J. Phys.: Condens. Matter **14**, 12063 (2002).
[30] A. Santos, Phys. Rev. E **86**, 040102(R) (2012).
[31] H. Reiss, H. L. Frisch, and J. L. Lebowitz, J. Chem. Phys. **31**, 369 (1959).
[32] J. L. Lebowitz, E. Helfand, and E. Praestgaard, J. Chem. Phys. **43**, 774 (1965).
[33] M. Mandell and H. Reiss, J. Stat. Phys. **13**, 113 (1975).
[34] Y. Rosenfeld, J. Chem. Phys. **89**, 4272 (1988).
[35] M. Heying and D. S. Corti, Fluid Phase Equilib. **220**, 85 (2004).
[36] K.-K. Han, J. H. Cushman, and D. J. Diestler, J. Chem. Phys. **93**, 5167 (1990).
[37] D. M. Heyes, Chem. Phys. **159**, 149 (1992).